Structural behaviour of super-light structures

Anne BAGGER[1*], Kristian Dahl HERTZ [2]

[1*] Department of Civil Engineering, Technical University of Denmark
Building 118, DTU, 2800 Kgs. Lyngby, Denmark
aeb@byg.dtu.dk

[2] Department of Civil Engineering, Technical University of Denmark

Abstract

A new structural concept, called *Super-light Structures* (SLS), has recently been invented and patented at the Technical University of Denmark. The basic concept of SLS is to construct a skeleton of a stiff and strong material, such as ordinary or high strength concrete, and stabilize this skeleton with a lighter and softer material, such as lightweight concrete. The combined use of stiff and light material in SLS results in structures of high stiffness and low weight. The applied technology and the advantages of SLS are elaborated upon in [1] in these proceedings. The present paper focuses on the structural correlation between the stiff material and the light material. The shape of the skeleton can be optimized for the primary load on the structure, and it will take up the majority of the load. The lighter material forms the outer geometry of the structural component (e.g. a wall), and has several structural functions: it leads load to the skeleton, it stabilizes the compression members of the skeleton, and it redistributes loads that are not optimal for the skeleton shape. In this paper, FE analysis is used to investigated the behaviour of a series of SLS beams of concrete, under varying stiffness and loading conditions.

Keywords: Super light structures, optimal structures, concrete, finite element

1 Introduction

The concept of Super-light Structures (SLS) is to combine a stiff, strong material – applied as the primary load carrying part of a given structural component – with a softer, lighter material, to stabilize and protect the stronger part [2]. The material is mainly thought as concrete; the strong part is an ordinary or high strength concrete, and the light material is a light aggregate concrete or a foam concrete. The SLS concept is invented and patented at the Technical University of Denmark [3] [4].
[1] in these proceedings presents the SLS concept, and its main advantages. An example of a possible SLS structure is shown in Figure 1.

The strong concrete in an SLS component is shaped as an optimized "skeleton" embedded in the light concrete. Skeleton parts which are subjected to tension in the structure are prestressed with prestressing wires, so that tension in these parts is taken by unloaded compression. The resulting structural component has a high stiffness to weight ratio, partly because the concrete is not cracked (high stiffness), and partly

because the heavy parts of the structure are only located in those areas where the forces are large (low weight).

Figure 1: Students' project using SLS. Skywalk in Oman. J.J. Sørensen and Z.A. Najafi.

The shape of the skeleton can be optimized with respect to the predominant load case. As for all minimal structures, this poses the question of the structure's behaviour for other load cases than the one it has been optimized for. *How sensitive is the structure to conditions (loads, geometry, materials, support settlements, etc.) that are different from the conditions it has been designed for.*

The aim of this paper is to investigate the sensitivity of a given SLS beam with regards to load conditions and skeleton geometry. A concrete SLS beam with a span of 20 meters and a height of 2 meters has been analyzed by finite element analysis (FEA) for 3 different skeleton configurations. Each of these have been subjected to two different load cases – a uniformly and a non-uniformly distributed load. Also, the stiffness ratio between the applied materials has been varied, to investigate how stresses redistribute in the beam due to a greater amount of creep in the light concrete than in the strong concrete. The results from these analysis are compared to each other, as well as to simple hand estimates of the involved forces.

The investigation shows that the SLS beam's behaviour is relatively insensitive to deviations between the most optimal skeleton shape and its actual shape, and that load situations other than the primary load do not lead to large stresses in neither the strong nor the light material. This means that the SLS is versatile in use, and that production considerations may play a significant role in designing the best shape of the skeleton.
Also, the investigation shows that hand calculations may provide good estimates of the largest stresses in the strong concrete. Further research must look more into how stresses in the light concrete can be estimated with adequate precision.

2 Method of analysis

An SLS beam with a span of 20 meters and a height of 2 meters has been analysed using FE software Abaqus. Three different geometric variations have been analysed, each with a different skeleton shape. The three geometric variants are shown in Figure 2, and are in the following referred to as *GeoA*, *GeoB* and *GeoC*. The shown section is uniform throughout the width of the beam, which is 0.2m.

The arched part of the skeleton in *GeoA* is a section of a circle. This is the one of the three skeleton shapes which is closest to the optimal shape for a uniformly distributed load, if the structure had only consisted of the skeleton itself (in which case the skeleton shape would be parabolic).

In *GeoB* the skeleton is created using a spline. The inclination of the arch is increased at the supports, and the middle part of the arch is almost straight.

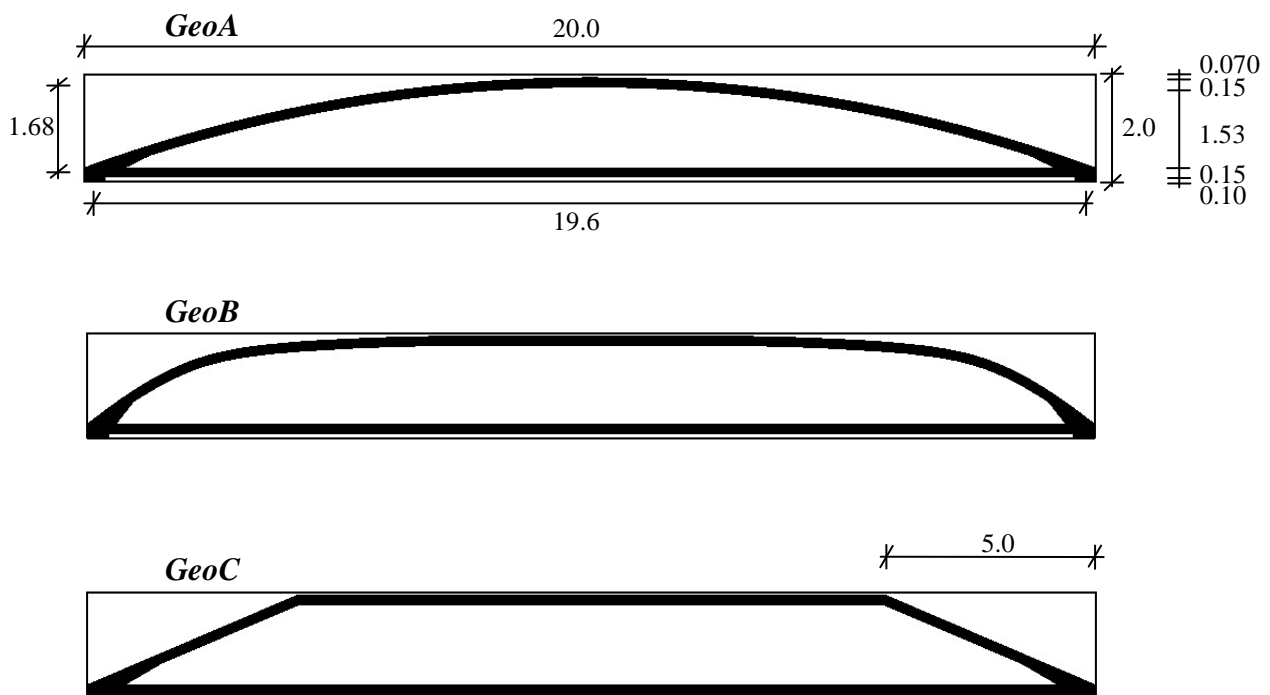In *GeoC* the skeleton consists of straight segments.

Figure 2: Geometric variants of SLS beam analysed in Abaqus. All measures in meters. The beam width is 0.2m.

Each beam consists of two materials; a stiff material (black areas in Figure 2) and a more flexible material (white areas in Figure 2). Each geometric variation has been analysed for two combinations of stiffnesses – the relevant values are listed in Table 1.

Table 1: E-modulus and poisson's ratio used in FE models.

Model	Geometry	E_{stiff} (10^3 N/mm^2)	ν_{stiff} $(-)$	E_{light} / (10^3 N/mm^2)	ν_{light} $(-)$
GeoA_INIT	GeoA				
GeoB_INIT	GeoB	35	0.2	2.0	0.2
GeoC_INIT	GeoC				
GeoA_CREEP	GeoA				
GeoB_CREEP	GeoB	17.5	0.2	0.5	0.2
GeoC_CREEP	GeoC				

The stiff material is a concrete of grade 40/50, and the light material is a light aggregate concrete. The two combinations in Table 1, INIT and CREEP, corresponds to the initial stiffness of the materials and the stiffness after some creep has occurred, respectively. Creep is modelled by repeating the linear elastic calculation, while using a reduced E-modulus which is inversely proportional to the strain increase due to the creep. In the creep combination in Table 1, the E-modulus of the stiff material is reduced by 50% and the E-modulus of the light material is reduced by 75%.

All calculations are linear elastic, and the material stiffness is assumed the same in tension and compression. This assumption is valid for the tension-zone in the skeleton if the applied prestress exceeds the calculated tension stress. The light concrete is assumed to be uncracked. The materials are modelled as isotropic. The calculations are linear, corresponding to an assumption of small deflections. A plain stress state is assumed.

The beams have been modelled by 4-node shell elements in Abaqus with a constant thickness of 0.2 meters. In areas of stress concentrations, the element size has been reduced until a further halving of the element size leads to an increase in the calculated stress of less than 10%. There are typically 3 elements across the thickness of the stiff skeleton parts.

Two load combinations have been analysed for all models: a uniform load case, where a vertical uniform line load of 1 kN/m (directed downwards) is acting on the entire beam, and a non-uniform load case, where the same load is acting on only the right half of the beam.

The beams are supported via equilateral triangles with a side-length of 0.4 meters (see Figure 3), and these are supported against translations at their down-pointing corner. In the right end of the beam, the support does not restrain movements in the beams longitudinal direction. This way, the beams are modelled as simply supported, with a contact width of 0.4 meters at the supports.
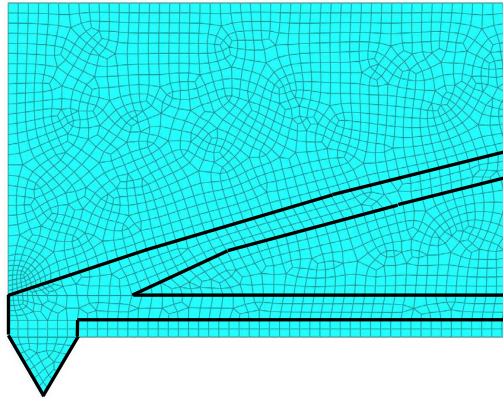
Figure 3: Part of GeoA, illustrating mesh and the supporting triangle. The marked area is modelled as concrete grade 40/50, the rest as a light aggregate concrete.

3 Results

3.1 Data from FE-analysis

Stresses and deflections in the analysed models can be found in Tables 2 and 3. Table 2 presents the results for the uniform load case, and Table 3 for the non-uniform load case. The presented results are normalised using the width of the beam, *b = 0.2m*, and the load, *p = 1kN/m*, since the results are proportional to these two parameters. The location of the presented stress parameters is illustrated in Figure 4.
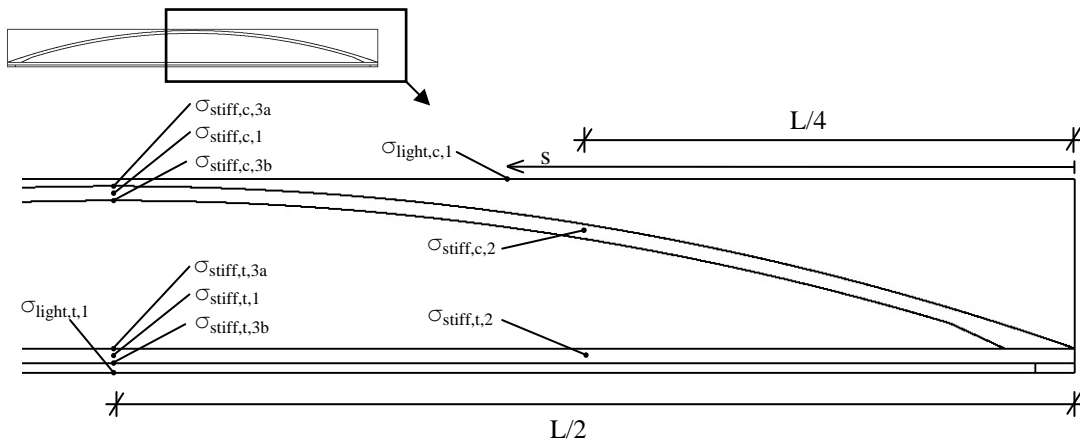

Figure 4: Location of the stress parameters presented in Tables 2 and 3.

In Figure 4, σ_{stiff} and σ_{light} refer to stresses in the strong, stiff concrete and the light concrete respectively. $\sigma_{xx,t}$ and $\sigma_{xx,c}$ refer to the maximal and minimal principal stress respectively (i.e. the largest tension stress and the largest compression stress). $\sigma_{xx,max}$ is the global maximum of the stress parameter in question. L is the beam length and *s* is the distance from the right end of the beam to the largest compression stress in the upper surface of the beam.

Table 2: Results from FE analysis of SLS beams for uniform load. b = 0.2m. p = 1kN/m.

UNIFORM LOAD			
	GeoA	GeoB	GeoC
Initial state (before creep, E_{stiff} / E_{light} = 17,5)			
u_{max} / b * 1000	7.7	6.5	6.7
Concrete 40/50			
$\sigma_{stiff,c,1}$ * b/p	-169	-169	-169
$\sigma_{stiff,c,2}$ * b/p	-132	-135	-111
($\sigma_{stiff,c,3a}$ - $\sigma_{stiff,c,3b}$) * b/p	-28	-33	-31
$\sigma_{stiff,c,max}$ * b/p	**-183**	**-186**	**-238** [2]
$\sigma_{stiff,t,1}$ * b/p	168	168	169
$\sigma_{stiff,t,2}$ * b/p	155	133	114
($\sigma_{stiff,t,3a}$ - $\sigma_{stiff,t,3b}$) * b/p	-28	-29	-30
$\sigma_{stiff,t.max}$ * b/p	**182**	**183**	**184**
Light aggregate concrete			
$\sigma_{light,c,1}$ * b/p	-17.0	-12.0	-13.8
s / L	0.20	0.50	0.38
$\sigma_{light,c,max}$ * b/p	**-21** [1]	**-12.0**	**-16.6** [1]
$\sigma_{light,t,1}$ * b/p	12.3	11.8	11.8
$\sigma_{light,t,max}$ * b/p	**12.3**	**11.8**	**11.8**
After creep (E_{stiff} / E_{light} = 35)			
u_{max} / b * 1000	17.4	14.5	14.9
Concrete 40/50			
$\sigma_{stiff,c,1}$ * b/p	-177	-179	-179
$\sigma_{stiff,c,2}$ * b/p	-153	-137	-133
($\sigma_{stiff,c,3a}$ - $\sigma_{stiff,c,3b}$) * b/p	-29	-40	-36
$\sigma_{stiff,c,max}$ * b/p	**-192**	**-199**	**-312** [2]
$\sigma_{stiff,t,1}$ * b/p	180	177	177
$\sigma_{stiff,t,2}$ * b/p	168	141	120
($\sigma_{stiff,t,3a}$ - $\sigma_{stiff,t,3b}$) * b/p	-29	-34	35
$\sigma_{stiff,t.max}$ * b/p	**195**	**194**	**195**
Light aggregate concrete			
$\sigma_{light,c,1}$ * b/p	-11.1	-6.6	-8.9
s / L	0.18	0.50	0.17
$\sigma_{light,c,max}$ * b/p	**-15** [1]	**-6.6**	**-11.6** [1]
$\sigma_{light,t,1}$ * b/p	6.2	6.4	6.4
$\sigma_{light,t,max}$ * b/p	**6.2**	**6.4**	**6.4**

Table 3: Results from FE analysis of SLS beams for non-uniform load. b = 0.2m. p = 1kN/m.

NON-UNIFORM LOAD			
	GeoA	GeoB	GeoC
u_{max} / b * 1000	4.0	3.3	3.4
Concrete 40/50			
$\sigma_{stiff,c,1}$ * b/p	-84	-86	-86
$\sigma_{stiff,c,2}$ * b/p	-88	-85	-81
$(\sigma_{stiff,c,3a} - \sigma_{stiff,c,3b})$ * b/p	-13	-19	-19
$\sigma_{stiff,c,max}$ * b/p	**-106**	**-104**	**-161** [2]
$\sigma_{stiff,t,1}$ * b/p	83	86	84
$\sigma_{stiff,t,2}$ * b/p	104	68	78
$(\sigma_{stiff,t,3a} - \sigma_{stiff,t,3b})$ * b/p	-13	-15	-18
$\sigma_{stiff,t.max}$ * b/p	**117**	**103**	**104**
Light aggregate concrete			
$\sigma_{light,c,1}$ * b/p	-11.8	-6.6	-9.8
s / L	0.19	0.36	0.38
$\sigma_{light,c,max}$ * b/p	**-15.4** [1]	**-6.6**	**-12.8** [1]
$\sigma_{light,t,1}$ * b/p	5.8	5.8	5.4
$\sigma_{light,t,max}$ * b/p	**7.6**	**6.8**	**6.8**
After creep (E_{stiff} / E_{light} = 35)			
u_{max} / b * 1000	9.0	7.5	7.7
Concrete 40/50			
$\sigma_{stiff,c,1}$ * b/p	-90	-88	-90
$\sigma_{stiff,c,2}$ * b/p	-101	-90	-90
$(\sigma_{stiff,c,3a} - \sigma_{stiff,c,3b})$ * b/p	-17	-23	-18
$\sigma_{stiff,c,max}$ * b/p	**-116**	**-112**	**-212** [2]
$\sigma_{stiff,t,1}$ * b/p	92	89	81
$\sigma_{stiff,t,2}$ * b/p	113	94	83
$(\sigma_{stiff,t,3a} - \sigma_{stiff,t,3b})$ * b/p	-16	-16	-15
$\sigma_{stiff,t.max}$ * b/p	**128**	**111**	**112**
Light aggregate concrete			
$\sigma_{light,c,1}$ * b/p	-7.7	-3.7	-6.4
s / L	0.18	0.36	0.17
$\sigma_{light,c,max}$ * b/p	**-11.0** [1]	**-3.7**	**-9.0** [1]
$\sigma_{light,t,1}$ * b/p	3.1	3.2	3.0
$\sigma_{light,t,max}$ * b/p	**4.2**	**3.6**	**3.6**

Notes to Tables 2 and 3

General: Unless something else is mentioned (note 1 and 2), $\sigma_{stiff,c,max}$ is located in the upper side of the compression arch, $\sigma_{stiff,t,max}$ is located in the underside of the strong concrete's tension zone, $\sigma_{light,c,max}$ is located at the upper surface of the beam, and $\sigma_{light,t,max}$ is located in the underside of the beam.

Note 1: The global compression stress maximum $\sigma_{light,c,max}$ is located at the vertical beam end, (for non-uniform load: in the loaded end of the beam), just above the compression arch.

Note 2: The global compression stress maximum $\sigma_{stiff,c,max}$ is located at the sharp angle-change in the compression "arch" (for non-uniform load: in the loaded part of the beam), on the underside of the "arch".

3.2 Comparison of results

Stresses in strong concrete:

→ The largest stresses in the strong concrete occur for the uniform load case.

→ The maximum compression force in the arch (i.e. compression stresses in the arch, summed up over the arch thickness) is almost the same for all three arch shapes.

→ The maximum compression force in the arch increases in the "after creep state" compared to the "initial state". The increase is 5-10%.

→ The largest tension force in the tension zone (i.e. tension stresses in the strong concrete, summed up over the thickness of the tension zone) is almost equal to the largest compression force in the arch.

→ For *GeoA* and *GeoB* the stress variation in the strong concrete over a vertical section in the arch or tension zone is 8-13% of the average stress in that section. This also applies for *GeoC*, except at the sharp angle-change in the compression zone.

→ *GeoC* has a stress concentration at the sharp angle-change in the compression zone. The stress in that point is 30-90% larger than the maximum stress in the compression zone in *GeoA* and *GeoB*.

Stresses in light concrete:

→ The largest stresses in the light concrete occur for the uniform load case.

→ The largest tension stress in the light concrete is 11-16% larger than the largest tension stress in the strong concrete, multiplied by the ratio between the E-modulus of the light and the strong concrete.

→ The largest compression stress in the light concrete is up to 230% larger than the largest compression stress in the strong concrete, multiplied by the ratio between the E-modulus of the light and the strong concrete.

Deflections:

→ The maximum deflection is comparable for the three geometric layouts, for a given load and material stiffness. The deflections are largest in *GeoA*.

→ In the "after creep state", where E_{stiff} is reduced by 50% and E_{light} is reduced by 75%, the deflections are increased by about 125%.

Figure 5 shows the largest compression stresses in *GeoA* for uniform and non-uniform load respectively. The top half of the figure shows both concrete materials, and the contour scale (top, left) is identical for the uniform and the non-uniform load. The lower half of the figure shows only the light concrete, and also here the contour scale (bottom, left) is identical for the two load cases. The figure illustrates some of the points given above.
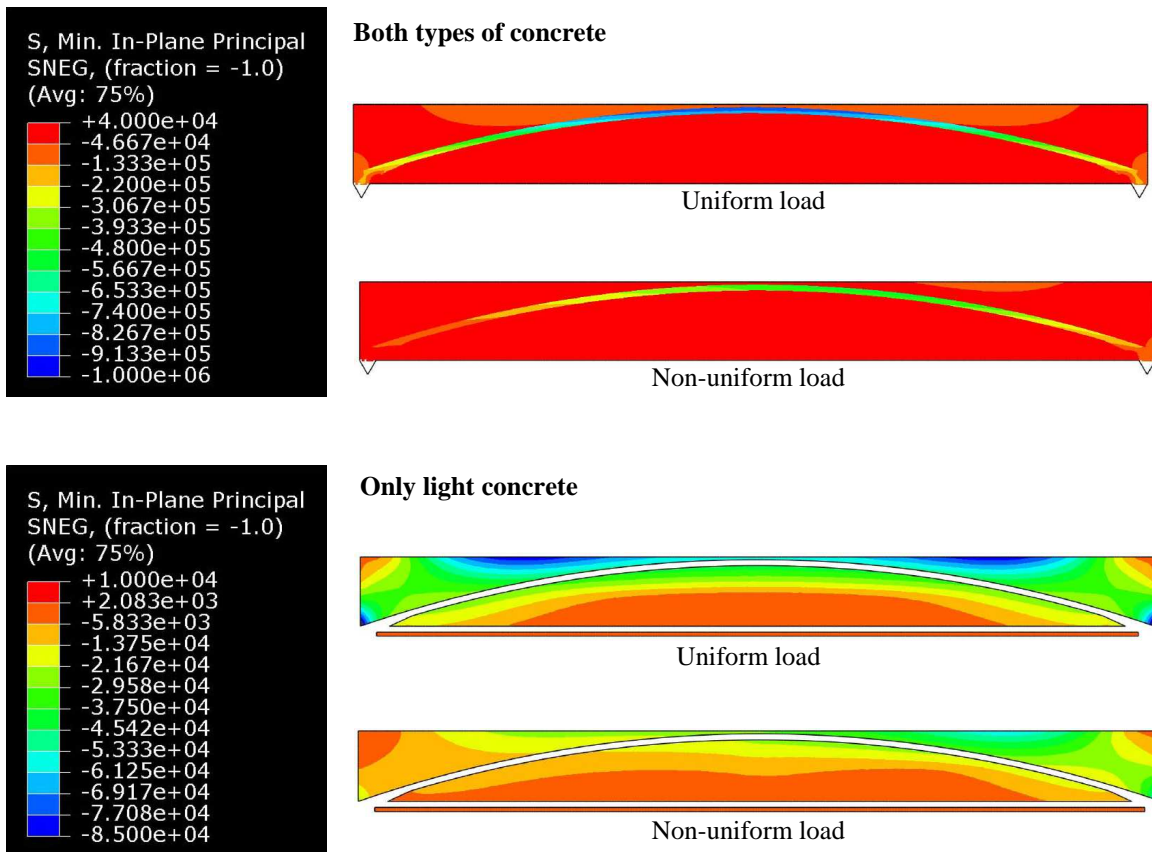

Figure 5:Minimum principal stress (i.e. largest compression stress) in N/m². The model is GeoA, initial state. Results are shown for uniform and non-uniform load.

3.3 Estimated values

In the following, a simple approximate calculation is performed to estimate the forces in the skeleton of the analyzed SLS beam. The estimate does not include the stiffness of the light concrete. The result of the estimate is compared to the results of the FE analysis.

For all three geometries, the distance between the center of the compression zone and the tension zone in the strong concrete is $a = 1.68$ meters and the span between the supporting triangles is $l = 19.6$ meters (see Figure 2). The height of the compression/tension zone is $h = 0.15$ meters. We get for a uniformly distributed load, p, when the beam width is b:

$$-\sigma_{stiff,c,1} * \frac{b}{p} = \sigma_{stiff,t,1} * \frac{b}{p} = \frac{l^2}{8ah} = \frac{(19.6m)^2}{8*1.68m*0.15m} = 190 \tag{1}$$

$\sigma_{stiff,c,1}$ is defined in Figure 4 as the compression force in the middle of the compression zone at the middle of the beam, and $\sigma_{stiff,t,1}$ is the equivalent stress in the tension zone. The stress is found by calculating the bending moment in the beam, and dividing this by the distance between the compression and tension zone, and by the cross sectional area of the compression/tension zone.

By comparing (1) to the information in Table 2, it can be seen that the FE analysis yields results that are 11% lower than estimated in (1) in the initial state (before any creep has taken place), and 6% lower after the given amount of creep has occurred.

4 Discussion

As stated in Section 3, the largest stresses in both the strong and the light concrete occur for the uniform load. This applies for all the analyzed geometric variants, and for both applied combinations of stiffness values (before and after creep). This suggests that an SLS beam like the one studied here, can be subjected to several load variations, and only be calculated for one: a load case where the largest distributed load on the beam is acting on the entire beam. It must be noted that concentrated forces have not been in focus in the present study.

The load case where a uniformly distributed load is acting on the entire beam, may be assessed by using a simple hand estimate: the stress in the skeleton parts is found by calculating the bending moment in the beam, and dividing this by the distance between the compression and tension zone in the skeleton, and by the cross sectional area of the compression/tension zone. In the present study, the larger the difference between the stiffness of the two concrete materials, the better the precision of the estimate.

Generally in the present investigations, the largest stresses in the strong concrete are independent of the skeleton shape. Only for the skeleton, which has a sharp angle in the arch (*GeoC*), a stress concentration occurs. This implies that other criteria than the statically optimal arch shape may be relevant in the design of the skeleton. Geometric criteria, such as room for openings in a wall, may influence the arch shape, or criteria connected to economical production methods. Further research could set up geometric

limits for "allowable" skeleton shapes, defined so that the stresses in the skeleton will not significantly exceed those in the statically optimal skeleton.

The stresses in the light concrete are related to the stresses in the strong concrete, and to the ratio between the stiffness of these materials (the E-modulus ratio). The largest stresses in the light concrete occur before any creep has taken place. In the analyzed beams, the largest tension stresses are lower than the largest compression stresses.

It is difficult to assess the compression stresses in the light concrete in a given SLS beam, as stress concentrations may occur, depending on the geometric layout. Compression stresses up to 230% larger than the largest compression stress in the strong concrete, multiplied by the E-modulus ratio, have been observed in the present study.

The largest observed tension stress in the light concrete is 11-16% larger than the largest tension stress in the strong concrete, multiplied by the E-modulus ratio. Other geometric layouts may increase the largest tension stress, especially if parts of the light concrete are cut away for window openings etc.

Since it is unlikely that the full design load will be applied to the beam simultaneously, some creep will have occurred before full load is reached. Therefore, analysis done on a beam in the initial state (before any creep has occurred) will yield conservative results for the stresses in the light concrete.

4.1 Future work

The stability of the compressed parts of the skeleton is secured by the light concrete. However, it must be assessed whether the light concrete provides the necessary resistance, for example concerning the adhesion between the materials in the contact surfaces between strong and light concrete.

Also, further analysis should be made to extend the validity of the present study's findings to other beam geometries (such as other skeleton shapes, other span-to-height ratios etc.) and other material stiffness values. As suggested above, the structural behaviour for concentrated loads should be studied, and further research should be made into the stresses in the light concrete.

5 Conclusion

An SLS beam was analyzed for three different skeleton shapes, two different combinations of material stiffness values (before and after creep), and two different load cases (a uniformly and a non-uniformly distributed load).

For the analyzed variants, the following was found:

→ The largest stresses in both skeleton and light concrete occurred for the uniformly distributed load.

→ The stresses in the skeleton were largely independent of the skeleton shape, and could be estimated with relatively good precision by a simple hand calculation.

→ The largest tension stresses in the light concrete were largely proportional to the largest tension stresses in the skeleton. The compression stresses were more autonomous, due to some stress concentrations.

References

[1] Hertz KD and Bagger A. Super-light structures with pearl-chain reinforcement. *Spatial Structures – Permanent and Temporary*. Shanghai, China, 2010. International Association for Shell and Spatial Structures (IASS).

[2] Hertz KD. Super-light concrete with pearl-chains. Magazine of Concrete Research 61, No.8. 655-663. Thomas Telford Ltd. October 2009.

[3] Hertz KD. "Light-Weight Load-Bearing Structures" (Super-light Structures). Application no. EP 07388085.8. European Patent Office, Munich. November 2007. Application no 61/004278 US Patent and Trademark Office. November 2007. PCT (Patent Cooperation Treaty) Application PCT/EP2008/066013, 21. November 2008. Patent January 2010.

[4] Hertz KD. "Light-weight load-bearing structures reinforced by core elements made of segments and a method of casting such structures" (Pearl-Chain Reinforcement). Application no. EP 08160304.5. European Patent Office, Munich. July 2008. Application no 61/080445 US Patent and Trademark Office. July 2008. PCT (Patent Cooperation Treaty) Application PCT/EP2009/052987, 13. March 2009. (Patent pending).